Available online at www.sciencedirect.com
ScienceDirect
International Journal of Mass Spectrometry 255–256 (2006) 123–129
www.elsevier.com/locate/ijms

Electron affinities of polynuclear aromatic hydrocarbons and negative-ion chemical-ionization sensitivities

L.D. Betowski [a,*], Mark Enlow [b], Donald H. Aue [c,**]

[a] U.S. Environmental Protection Agency, NERL, P.O. Box 93478, Las Vegas, NV 89193, United States
[b] Applied Research Associates Inc., P.O. Box 40128, Tyndall AFB, FL 32403, United States
[c] Department of Chemistry, University of California, Santa Barbara, CA 93106, United States

Received 28 October 2005; received in revised form 24 April 2006; accepted 24 April 2006
Available online 5 June 2006

Abstract

Negative-ion chemical-ionization mass spectrometry (NICI MS) has the potential to be a very useful technique in identifying various polycyclic aromatic hydrocarbons (PAHs) in soil and sediment samples. Some PAHs give much stronger signals under NICI MS conditions than others. On the other hand, positive-ion signals are largely comparable under the same source conditions. An extensive set of newly re-evaluated experimental electron affinities (EAs), or free energies of electron attachment, are now available, as well as reliable predicted electron affinities from quantum theoretical calculations or from solution reduction potentials and theoretically predicted solvation energies. In order to show a high negative-ion sensitivity, a PAH must have an EA that exceeds a threshold of approximately of 0.5 eV. Comparisons between the negative-ion to positive-ion sensitivities (*N*/*P* ratios) and these new electron affinities show a rough correlation between the two, but naphthacene and perylene are exceptions to this relationship with much lower sensitivities than expected from their high EA values. By calculating the EA for a PAH, one can predict whether a sensitivity enhancement under NICI MS conditions is to be expected. Since aliphatic hydrocarbons and many other substances have negative or very low EAs, NICI MS is expected to be a good technique for detecting PAHs in samples contaminated with other hydrocarbons or compounds with low EAs.

Keywords: Polynuclear aromatic hydrocarbon (PAH); Electron affinity; Chemical-ionization mass spectrometry; Computational chemistry

1. Introduction

Polycyclic aromatic hydrocarbons (PAHs) [1–3] have been implicated as comprising one of the largest classes of environmental carcinogens [4–6]. Recent attempts at natural attenuation [7] have led to renewed interest in methods for the analysis of PAHs in different soil types, and the U.S. Environmental Protection Agency (EPA) continues to be interested in developing methods for the detection of PAHs. One determinative method for the detection of PAHs that minimizes interferences due to aliphatic hydrocarbons is chemical-ionization (CI) mass spectrometry. We have previously measured absolute response factors with negative-ion and positive-ion chemical ionization in methane and found enhanced negative-ion sensitivity for various PAHs and other environmentally important molecules, thereby minimizing chemical noise [8]. For a dramatic example, the carcinogen, benzo[*a*]pyrene, shows a negative-ion CI signal about 1000 times larger than that for its non-toxic isomer, benzo[*e*]pyrene [9–11]. The enhanced negative-ion sensitivities are often measured relative to the corresponding chemical-ionization positive-ion signal or electron-impact signal (*N*/*P* ratio), rather than as an absolute response factor [11].

In prior work, we have carried out a series of calculations with different quantum mechanical methods to determine proton affinities (PAs) of PAHs and found that the theoretical PAs reproduced experimental values with standard errors between 1.36 kcal mol^{-1} (0.06 eV) and 2.12 kcal mol^{-1} (0.09 eV) [12]. Knowledge of the PAs of the PAHs to be analyzed can be used to produce a strong specificity in response factors under positive-ion chemical-ionization conditions. With methane as a CI gas, all PAHs are expected to show similar response factors.

---

[*] Corresponding author. Tel.: +1 702 798 2116; fax: +1 702 798 2142.
[**] Corresponding author. Tel.: +1 805 893 2643; fax: +1 805 893 4120.
E-mail addresses: betowski.don@epa.gov (L.D. Betowski), aue@chem.ucsb.edu (D.H. Aue).

1387-3806/$ – see front matter © 2006 Elsevier B.V. All rights reserved.
doi:10.1016/j.ijms.2006.04.008

With ammonia gas, however, PAHs with PAs higher than that of ammonia, show a high CI sensitivity while PAHs with lower PAs show little or no signal [13].

Previously, it had been suggested that the highly variable negative-ion sensitivity might be related to the electron affinity of the sample [8,11,14], and correlations for PAHs were found with EAs estimated by Hückel or semiempirical molecular orbital theory [14,15] or taken from the experimental literature. We have recently published a thorough re-evaluation of the known experimental EAs for 45 PAHs and related compounds in the light of the EAs estimated from calculations by various quantum theoretical methods. Furthermore, EAs of these PAHs could be closely predicted from solution reduction potentials of the PAHs together with solvation energies estimated from the Born solvation terms of the radical anions [16]. This analysis resolved inconsistencies between different experimental EAs and experimental EAs that appeared to be significantly in error. The most effective quantum theoretical methods involved the use of density functional theory (DFT), using the B3LYP method and 6-311G(d,p) or 6-31 + G(d,p) basis sets, with standard errors of 0.077 and 0.070 eV, respectively, when compared with reliable experimental EA data. The other method for estimation of EAs from solution reduction potentials gives standard errors of 0.075 eV. Armed with this newly revised set of experimental EAs and two independent methods to predict EAs for PAHs for which experimental data are lacking, we set out here to test the idea that negative-ion sensitivities might be related to electron affinity.

2. Theoretical methods

EAs are more difficult to calculate than PAs and IPs for a number of reasons. PAs generally involve calculations of even-electron, closed-shell systems. EAs generally involve odd-electron systems where spin contamination and scf convergence problems, especially with diffuse functions, add to the difficulty of producing reliable results. IPs also involve odd-electron systems, but Koopmans' theorem methods [17], which equates the IP to the energy of the highest occupied molecular orbital (HOMO), give reasonable approximations to this energy. Koopmans' theorem can also be used to approximate EAs with the energies of the lowest unoccupied molecular orbitals (LUMO), but is less effective than for IPs. Whereas for IPs, the Koopmans' theorem results are close to experiment because of a fortuitous cancellation of electron-correlation and ion-relaxation terms; for EAs there is no such cancellation but an addition of these terms [18].

The methods used have been discussed in detail previously [16]. Since available experimental electron affinities of PAHs are largely adiabatic, the most direct theoretical method comes from calculation of the energies of both the neutral and anionic forms of the PAH at their respective optimized geometries, the "ΔE" method. All calculations were performed using the Gaussian 94, Gaussian 98 and Gaussian 03 program suites [19].

Geometries for the neutral and anionic forms at the B3LYP/6-311G(d,p) level were used, and frequency calculations carried out in order to verify that the stationary points thus obtained were true minima and to determine thermodynamic parameters for the determination of reaction energetics. Thermochemical data were calculated with zero-point and thermal energy corrections from scaled B3LYP/6-311G(d,p) frequencies using a scaling factor of 0.99 derived from linear regressions of DFT zero-point energies with experimentally known zero-point energies of organic molecules [20]. A scaling factor of 0.96 for DFT frequencies for the thermal and entropy terms was derived from linear regressions on experimental frequencies of organic molecules and PAHs [20]. Single-point B3LYP/6-31 + G(d,p) calculations at the B3LYP/6-311G(d,p) geometries were carried out to account for the effect of diffuse functions on reaction energetics using the scf = tight option in Gaussian. For the open-shell radical anions, all calculations were done with spin-unrestricted methods, where spin contamination from quartet and higher spin states is a potential problem. With the UB3LYP method S^2-values (from 0.76 to 0.77) were close to the expected 0.75 value for a pure doublet spin state. Spin-restricted ROB3LYP calculations generally raised the energies of the anions by about 0.03 eV [16].

Details of geometries, molecular symmetries, thermodynamic data and electronic energies are reported in the supplemental material for this paper and for Ref. [16]. Some of the calculations were performed at the National Environmental Scientific Computing Center (NESCC) of the U.S. EPA.

3. Results and discussion

The negative-ion sensitivities for PAHs under chemical-ionization mass spectrometric conditions in methane have been measured directly by Oehme [10] and in our laboratories [8]. They have also been measured indirectly as negative-ion/positive-ion (*N*/*P*) ratios by the Daishima group [11]. For the *N*/*P* ratios to be used as a measure of negative-ion sensitivity, the positive-ion sensitivities must be known. When the thermodynamics are favorable, proton transfer from CH_5^+ to another molecule is found to occur on almost every collision, with the collision rate accurately predicted by the average-dipole-orientation (ADO) theory of Su and Bowers [21]. The rate depends on the polarizability and the dipole moment of the molecule and the reduced mass of the ion and molecule. While the ADO rate constants generally vary by no more than a factor of two, the response factors for PAHs show a somewhat larger variation [8]. Positive-ion CI response factors vary by a factor of 3 for eight PAHs and 10 for other molecules whose gas-phase basicities (GBs) cover a range up to 80 kcal mol^{-1} higher than the GB of methane. Rate constants measured for protonation of a variety of molecules with CH_5^+ show little variation and are well predicted by ADO theory [22]. Thus, positive-ion sensitivities can be considered to be nearly constant for PAHs, and the *N*/*P* ratios may, in fact, be used as a rough measure of negative-ion sensitivities.

Response factors in the negative-ion CI mode vary by a factor of 1000 and, for PAHs, by a factor of 350 [8]. Interpretation of these differences, however, is complicated by the fact that the negative-ion peaks result from parent ions, fragment ions, and proton-abstraction and net hydride-addition reactions. When

Table 1
N/*P* ratios and free energies for electron attachment for polycyclic aromatic hydrocarbons (energies in eV)

Compound	*N*/*P* ratio[a]	Base peak	$-\Delta G^\circ{}_{\mathrm{a,298,exptl}}$[b]	$-\Delta G^\circ{}_{\mathrm{a,ec,pred}}$[c]	$-\Delta G^\circ{}_{\mathrm{a,298}}$[d] QM calculated	$-\Delta G^\circ{}_{\mathrm{a,pred}}$[e] QM calculated
Indene	*0.005 (0.18)*	$(M-\mathrm{H})^-$	−0.4	−0.40	−0.35	−0.41
Azulene	64	M^-	0.81	0.79	0.80	0.65
Naphthalene	*0.0004 (0.006)*	$(M-\mathrm{H})^-$	−0.16	−0.10	−0.04	−0.12
1-Methylnaphthalene	*0.0006 (0.15)*	$(M-\mathrm{H})^-$	−0.2	−0.08	−0.02	−0.11
2-Methylnaphthalene	*0.0007 (0.13)*	$(M-\mathrm{H})^-$	−0.2	−0.10	−0.00	−0.09
Acenaphthylene	6.0	M^-	0.8	0.77	0.87	0.71
Biphenyl	*0.0003 (0.002)*	$(M-\mathrm{H})^-$	−0.1	−0.09	0.05	−0.05
Fluorene	*0.005 (0.31)*	$(M-\mathrm{H})^-$	−0.1	−0.12	−0.09	−0.17
Anthracene	2.9	M^-	0.60	0.60	0.71	0.57
Phenanthrene	0.020 (0.11)	$(M-\mathrm{H})^-$	0.1	0.10	0.17	0.07
1-Methylanthracene	6.0 (6.1)	M^-	0.55	0.64	0.70	0.56
Fluoranthene	8.1	M^-	0.7	0.83	0.89	0.73
Pyrene	0.22 (0.23)	M^-	0.56	0.53	0.60	0.47
Benz[*a*]anthracene	12.9 (13)	M^-	0.70	0.58	0.76	0.61
Benzo[*c*]phenanthrene	0.17 (0.27)	$M\mathrm{H}^-$	0.40	0.37	0.53	0.40
Chrysene	0.017 (0.12)	$(M-\mathrm{H})^-$	0.42	0.35	0.53	0.42
Naphthacene (tetracene)	0.52	M^-	1.02	0.97	1.23	1.05
Triphenylene	0.015 (0.10)	$(M-\mathrm{H})^-$	0.29	0.20	0.34	0.24
Benzo[*a*]pyrene	400	M^-	0.77	0.83	0.96	0.80
Benzo[*e*]pyrene	0.43 (0.46)	M^-	0.49	0.56	0.67	0.54
Perylene	1.5	M^-	1.00	0.97	1.14	0.97
Benzo[*ghi*]perylene	210	M^-	0.7	0.68	0.92	0.77
Picene	0.07 (0.08)	M^-	0.54	0.41	0.64	0.51
Dibenzo[*a*,*h*]anthracene	27	M^-	0.68	0.64	0.80	0.66
Coronene	16.9 (17)	M^-	0.57	0.67	0.86	0.71

[a] Data corrected for ^{13}C contribution [11]; numbers in parenthesis are uncorrected for ^{13}C contribution. Ratios in italics might be 0, within experimental error.

[b] Recommended experimental free energy values [16]. Numbers quoted to one decimal are predicted values [16].

[c] Predicted free energies from electrochemical Hg reduction potentials in Eq. (1), which includes solvation effects predicted from $1/r$ [16].

[d] Calculated at the B3LYP/6-31 + G(d,p) level [16].

[e] Predicted from the calculated B3LYP/6-31 + G(d,p) free energies from linear regression: $y = 0.9188(-\Delta G^\circ{}_{\mathrm{a,298}}) - 0.088$ [16].

only the PAHs with parent-ion peaks in this paper are considered, the variation is much smaller [8]. The much larger variety of PAHs in the work of Oehme [10], give primarily parent-ion peaks, with negative-ion methane CI response factors varying by a factors up to 10,000. A similarly large variation, up to 1000, is seen in the *N*/*P* ratios measured by Daishima under methane CI conditions [11]. While there is largely a semi-quantitative agreement between measurements in different laboratories, there are some significant unexplained differences, most notably between fluoranthene, benzo[*b*]fluoranthene, and pyrene [8,10,11].

Nevertheless, the *N*/*P* ratios measured by Daishima et al. provide the most complete and self-consistent set of data for PAHs. In Table 1, are *N*/*P* data for 26 PAHs for which experimental EAs or free energies of electron attachment are available. We compare these *N*/*P* ratios in Table 1 with experimental and theoretically predicted free energies of electron attachment to try to better understand the enhancement in the negative-ion signals for certain structures. Negative-ion sensitivity data have previously been compared with electron affinities, but before reliable experimental or theoretical data were available [11,14]. In our previous paper [16], we have found that nearly half of the experimental EAs in the literature were in error, many seriously. Thus, we include in Table 1 our recommended experimental free energies of electron attachment, $-\Delta G^\circ{}_{\mathrm{a,298,exptl}}$, critically evaluated in the light of reliable quantum mechanical calculations and our analysis of electrochemical reduction potentials [16]. In this table, the literature *N*/*P* ratios have been modified to measure only the parent M^- molecular ion peak, and have been corrected from Daishima's data for the ^{13}C contribution to the M^- peak from any $M-\mathrm{H}^-$ peak present. Thus, the *N*/*P* ratio refers to the $M^-/M\mathrm{H}^+$ ratio, even in cases where the M^- was not the base peak in the spectrum.

Table 1 shows a comparison of experimental EA data with data derived from the methods we have developed for predicting the EA values for molecules for which experimental data are not known. The $-\Delta G^\circ{}_{\mathrm{a,ec,precd}}$value is the predicted free energy from the electrochemical reduction potential, $E_{1/2}$ [23], and the solvation energy difference between neutral and ion from a Born electrostatic model utilizing the calculated molecular volume and a derived radius, *r*, for a pseudospherical ion according to Eq. (1) [16]:

$$-\Delta G^\circ{}_{\mathrm{a,ec,pred}} = \left[-5.6701\left(\frac{1}{r}\right) - 0.739\right] + E_{1/2} + 4.21 \quad (1)$$

The $-\Delta G^\circ{}_{\mathrm{a,298}}$ values in Table 1 are calculated at the B3LYP/6-31 + G(d,p) level, and $-\Delta G^\circ{}_{\mathrm{a,ec,pred}}$ values are predicted free energies from a linear regression fit of calculated free energies with reliably known experimental values according to Eq. (2) [16]:

$$-\Delta G^\circ{}_{\mathrm{a,ec,pred}} = 0.9188(-\Delta G^\circ{}_{\mathrm{a,298}}) - 0.088 \quad (2)$$

Table 2

N/*P* ratios and predicted free energies for electron attachment for polycyclic aromatic hydrocarbons for which experimental energies are not available (energies in eV)

Compound	*N*/*P* ratio[a]	Base peak	$-E_{1/2}$[b]	$-\Delta G^{\circ}_{\mathrm{a,ec,pred}}$[c]	$-\Delta G^{\circ}_{\mathrm{a,298}}$[d] QM calculated	$-\Delta G^{\circ}_{\mathrm{a,pred}}$[e] QM calculated	$-\Delta G^{\circ}_{\mathrm{a,pred}}$[f] QM calculated
Acenaphthene	0	$[M-\mathrm{H}]^-$	2.1	−0.23	−0.36	−0.21	−0.23
2-Methylanthracene	1.06	M^-	1.45	0.60	0.59	0.57	0.55
1-Methylphenanthrene	*0.011*	$[M-\mathrm{H}]^-$	1.94	0.11	0.06	0.14	0.10
9-Phenylanthracene	8.0	M^-	1.36	0.81	0.68	0.65	0.64
Benzo[*a*]fluorine	*0.004*	$[M-\mathrm{H}]^-$			0.22	0.27	0.24
Benzo[*b*]fluorine	*0.005*	$[M-\mathrm{H}]^-$			0.30	0.34	0.31
7-Methylbenz[*a*]anthracene	19	M^-	1.5	0.64	0.64	0.62	0.60
12-Methylbenz[*a*]anthracene			1.5	0.64	0.66	0.64	0.61
7,12-Dimethylbenz[*a*]anthracene			1.5	0.67	0.67	0.65	0.63
Benz[*a*]aceanthrylene (benzo[*a*]fluoranthene)			0.975	1.17	1.25	1.13	1.16
Benz[*e*]acephenanthrylene (benzo[*b*]fluoranthene)	220	M^-	1.375	0.77	0.85	0.80	0.81
Benzo[*j*]fluoranthene	32	M^-	1.165	0.98	1.07	0.98	1.00
Benzo[*k*]fluoranthene	150	M^-	1.39	0.76	0.85	0.79	0.79
Indeno[1,2,3,*cd*]pyrene	380	M^-	1.19	1.02	1.14	1.04	1.05
Dibenzo[*def*,*mno*]chrysene (anthanthrene)	210	M^-	1.19	0.98	1.28	1.15	1.17
Benzo[*b*]triphenylene (dibenz[*a*,*c*]anthracene)	25	M^-	1.53	0.66	0.69	0.66	0.65
Dibenzo[*b*,*def*]chrysene (dibenzo[*a*,*h*]pyrene)	360	M^-	1.16	1.06	1.19	1.08	1.09
Dibenzo[*a*,*e*]pyrene	280	M^-	1.36	0.86	0.89	0.83	0.83

[a] Data corrected for ^{13}C contributions [11a]. Ratios in italics might be 0, within experimental error.

[b] Experimental reduction potentials vs. Hg [23].

[c] Predicted free energies from electrochemical Hg reduction potentials in Eq. (1), which includes solvation effects predicted from $1/r$ [16].

[d] Calculated values at the B3LYP/6-311G(d,p) level.

[e] Predicted from the B3LYP/6-311G(d,p) level free energies from linear regression: $y = 0.8334 - \Delta G^{\circ}_{\mathrm{a,298}} + 0.087$ [16].

[f] Predicted from the B3LYP/6-31 + G(d,p) level free energies from linear regression: $y = 0.9188 - \Delta G^{\circ}_{\mathrm{a,298}} - 0.088$ [16].

In Table 1, the free energies of electron attachment predicted from electrochemical data and quantum mechanical calculations compare very well with one another and with the recommended experimental values, with standard errors in the regressions for Eqs. (1) and (2) of 0.075 and 0.070 eV, respectively, establishing the reliability of these two independent methods of prediction [16]. A nearly identical standard error, 0.077 eV, was established for B3LYP/6-311G(d,p)// B3LYP/6-311G(d,p) calculations on these PAHs as well [16].

We can now take advantage of the availability of these EAs to analyze negative-ion sensitivity data in Table 2 for PAHs for which experimental EAs are not available. In these cases, we have utilized quantum mechanical calculations at both the B3LYP/6-311G(d,p) and B3LYP/6-31 + G(d,p)// B3LYP/6-311G(d,p) levels in connection with the regression equations from our previous paper [16] to provide predicted free energies of electron attachment. We have included the independently predicted free energies of electron attachment from reduction potentials, where available. Also in Table 2 are three PAHs, two carcinogenic methylbenz[*a*]anthracenes and benz[*a*]aceanthrylene, for which *N*/*P* values are not known, but might now be predicted. Again, the predicted free energies from the two quantum mechanical methods and from experimental electrochemical data all compare very well with one another. In almost all cases, agreement is to within 0.1 eV, giving us enough confidence in the predicted free energies of electron attachment to use them to analyze the *N*/*P* data in Table 2 along with the data in Table 1.

From the patterns displayed in Tables 1 and 2, it appears that enhancement in the negative-ion intensity over the positive-ion intensity, i.e., to get $N/P > 1$, requires that the EA, or free energy of attachment, must reach a threshold value of about 0.5 eV. Several molecules, pyrene, chrysene, benzo[*e*]pyrene, benzo[*c*]phenanthrene, and picene, have borderline electron affinities and show *N*/*P* ratios somewhat less than 1. The various substituted anthracenes in Tables 1 and 2 have electron affinities close to the borderline and *N*/*P* ratios only a bit above 1. Molecules with free energies of electron attachment less than 0.30 eV generally have very low *N*/*P* ratios and base peaks in the negative-ion spectrum at $M-\mathrm{H}^-$, rather than M^-. In fact, almost all of these molecules, except for phenanthrene and triphenylene, have M^- intensities that, after ^{13}C correction from the $M-\mathrm{H}^-$ peak, are so near to zero that experimental errors could be large enough for the true intensities to actually be zero. This is almost surely the case for those with negative EAs and likely so for the others as well. The reported experimental intensities for phenanthrene and triphenylene appear to indicate real M^- peaks, but this is remarkable, given their low EAs. Other experimental data [11b,24] sometimes show parent molecular anion intensities barely above zero, after ^{13}C correction from the $M-\mathrm{H}^-$ peak, for these molecules and for pyrene, chrysene, benzo[*c*]phenanthrene, benzo[*e*]pyrene, and picene. In all of these molecules, the electron affinities are close to 0.5 eV, where there may be some doubt about whether molecular anions are truly formed. The relative intensities of the $M-\mathrm{H}^-$, and the corresponding ^{13}C correction to the parent peak, vary significantly, depending upon the exact experimental conditions. The experimental EAs for phenanthrene and triphenylene come from electron-capture detector (ECD) experiments, where mass measurements were not made for the ions formed, and the experimental EA data are therefore suspect, especially for

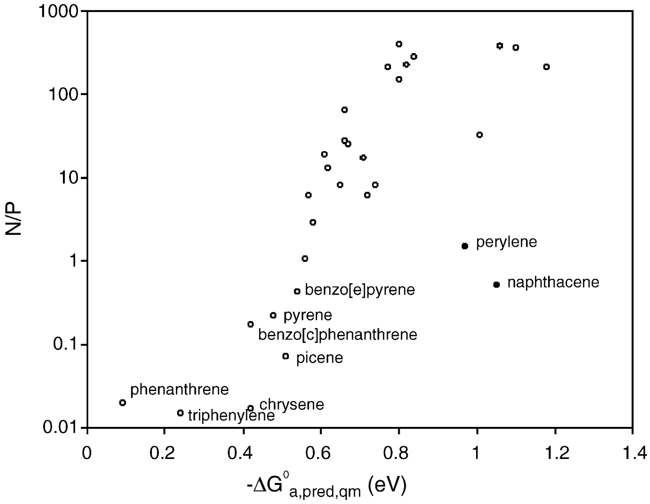

Fig. 1. Logarithmic plot of the negative-ion to positive-ion ratio vs. free energies for electron attachment predicted from B3LYP/6-31 + G(d,p) quantum mechanical calculations. The solid points are outliers and the other labeled points have *N*/*P* ratios that may be dubious, especially those with lowers free energies of attachment.

phenanthrene. ECD measurements of EAs have previously been demonstrated to be seriously in error in cases where the electron affinities are low [16], and in other cases as well [25,26]. For phenanthrene, we have tabulated as experimental values the estimated EAs from experimental electrochemical reduction potentials [16].

Nitrobenzene, 2,4-dintrotoluene, and 2,6-dinitrotoluene from the study by Betowski et al. [8], generate molecular anions and show enhanced response factors. Nitrobenzene and 2,6-dinitrotoluene have experimental EAs of 1.01 and 1.39 eV, respectively [27]. Another compound studied was isophorone. The NICI MS of this compound did not show any enhancement, plus the major ion seen in this mode was the $(M-\mathrm{H})^-$ at *m*/*z* 137. The EA for isophorone was calculated at −0.13 eV, consistent the fact that a parent ion was not observed.

Especially for PAHs with electron affinities above 0.5 eV, there appears to be a rough correlation between the *N*/*P* ratio and electron affinity. In Fig. 1, the logarithm of the *N*/*P* ratio is plotted versus the B3LYP/6-311G(d,p) regression-predicted free energy of electron attachment for 30 PAHs. The 10 PAHs for which the M^- ion intensity is most questionable (with *N*/*P* data in italics in Tables 1 and 2) were excluded from the plot. Most ions fall within 0.1–0.2 eV of a correlation line. There are two major exceptions, naphthacene and perylene. Ironically, these two compounds have the highest free energies of electron attachment, but the *N*/*P* ratios are only 0.52 and 1.5, respectively. How can the overall trend in the *N*/*P* ratios with increasing EA and the two major outliers be explained?

Previous research on negative-ion formation by electron attachment has shown that ions with electron affinities below about 0.5 eV generally cannot be detected mass spectrometrically [28,29]. For a limited number of molecules, rates of attachment in the high-pressure limit have been measured, showing very rapid rates when electron affinities are high [30,31]. Curiously, however, the correlation of the rate of attachment with electron affinity for a series of substituted nitrobenzenes is only rough, with several major outliers that cannot be explained by factors like dipole moment, steric effects, or entropy and geometry changes on ionization [28]. Density of state arguments were considered, but the existence of low-energy excited states of the ion to enhance the density of states did not explain all the outliers either. Thus, previous work in this field is consistent with the facts that we see in Fig. 1: a rough trend in the *N*/*P* ratio versus EA, but with major outliers, and a small or negligible *N*/*P* ratio for molecules with EAs below 0.5 eV. It seems clear that the explanation for these phenomena must reside in a better understanding of the factors affecting the rates of electron capture. At EAs above approximately 0.8 eV, it appears that the *N*/*P* versus EA linear plot may be leveling off at a maximum *N*/*P* ratio around 600. As we will see, however, the cross sections for electron attachment to C_{60} and C_{70}, with EAs of 2.7 eV, are especially large.

In the negative-ion chemical-ionization experiment, there are abundant thermalized electrons in the ion source. If the thermodynamics are favorable, a molecule will capture an electron at a rapid rate. Using the ADO theory, the rate constant is extremely fast due to the small reduced mass of a system consisting of an electron and a molecule. If the electron affinity is significantly positive, the reaction equilibrium for electron capture should be favorable, and one might expect to see a signal corresponding to formation of the parent molecular anion. In this context, however, there are additional factors that may complicate observation of a parent ion. Electron affinities are generally reported using the “stationary-electron approximation” [29]. The entropy and integrated heat capacity of the electron must be considered in determining the free energy for electron attachment at elevated temperatures, 375 K in Daishima’s experiments. The entropy of the electron at 350 K is 5.79 cal mol^{-1} K^{-1}, making $-T\Delta S^{\circ}$ equal to 0.088 eV at 350 K, and the integrated heat capacity is 0.075 eV, leading to a near cancellation of these two effects, with the free energy only 0.013 eV less favorable than expected from calculated free energies within the stationary-electron approximation [32]. Additionally, however, there are major problems in observing the parent ions from mildly exoergonic electron-attachment reactions. Slow electron-attachment rates and/or short lifetimes of these ions as a result of autodetachment of the electron prevent their collisional stabilization [28,33–35]. The observation of anions under high-pressure conditions has been shown to be complicated further by reactions of the ions with trace gas impurities like water and oxygen [36].

In flowing afterglow Langmuir probe (FALP) studies of PAH ionization cross sections as a function of electron energy, Tobita et al. [35] reported that it appeared that an EA ≥ 0.5 eV is required for the negative-ion states of PAHs to be long-lived. For PAHs with EAs less than 0.5 eV, the anionic states are too short-lived to allow the direct observation of the parent anion prior to its decay, mainly by autodetachment. They also found that formation of $(M-\mathrm{H})^-$ ions occurred at high electron energies (onset 5.5–6.2 eV) for phenanthrene and triphenylene. They did not study chrysene and benzo[*c*]phenanthrene. Since we expect thermal electrons (approximately 0.03 eV) to predominate under CI conditions, we do not expect the $(M-\mathrm{H})^-$ ions to be formed by fragmentation following the electron-capture process, but rather by proton abstraction by bases formed from chemical impurities, e.g., from OH^- ions originating from H_2O or O_2 [11].

In these experiments, the structure in the cross section versus electron energy curves showed evidence of resonances at electron energies above zero-electron energy that were attributed to electron-excited Feshbach resonances [35]. Consistent with the observation that naphthacene and perylene show extraordinarily low *N*/*P* ratios, they found that these two molecules were also exceptional in their cross section curves, showing no resonance, and very little ion formation, at zero-electron energy and resonances only at higher energies. Such behavior might be explained as the result of low Franck–Condon factors for ionization of these molecules, but we see no evidence of an unusually large geometry change for these ions compare to other PAH anions. Although these PAHs have high symmetry, D_{2h}, the ions have the same symmetry on the B3LYP/6-311G(d,p) surfaces.

The general trend of higher negative-ion sensitivity with higher electron affinity in PAHs may be explained by the expectation that the electron-attachment rates and collision lifetimes of the molecular anions will increase as the density of vibrational states in the ion increases, permitting rapid ion formation and collisional stabilization. It is expected that the density of states will increase dramatically as the electron affinity increases and the energy well corresponding to the anion gets deeper. This rough trend in both attachment rates and ion lifetimes has been verified experimentally for substituted nitrobenzenes [30]. We noted, in Fig. 1, that the *N*/*P* ratios might be beginning to level off for EAs above 0.8 eV. The rate data for nitrobenzenes, however, are not so consistent with this idea, since the rates continue to increase, albeit irregularly, up to 2 eV [30]. Furthermore, the cross sections for electron attachment to C_{60} and C_{70}, with EAs of about 2.7 eV, are unusually high compared to other PAHs [33,35].

The data in Fig. 1 and the nitrobenzene data [30], show outliers and a scatter in rates and *N*/*P* ratios. When the 26 PAHs in Fig. 1 with the highest EAs are considered, excluding the 10 PAHs with italicized *N*/*P* ratios, phenanthrene and triphenylene, and the outliers (naphthacene and perylene), a regression with free energies of electron attachment shows $R^2 = 0.66$ and a standard error in $\log N/P$ of 0.745, or a factor of 5.5 in *N*/*P*. Excluding the next 5 PAHs with low EAs, and somewhat dubious *N*/*P* ratios, gives a standard error corresponding to a factor of 3.6 in *N*/*P* ratio. For the two carcinogenic methylbenz[*a*]anthracenes and benz[*a*]aceanthrylene in Table 2, the predicted free energies of electron attachment can be used, in connection with these regressions, to make a prediction of an *N*/*P* ratio of about 15 for two carcinogenic methylbenz[*a*]anthracenes and 600 for benz[*a*]aceanthrylene. We suggest some caution in the prediction or interpretation of the *N*/*P* data, however, since considerable variation of *N*/*P* ratios and negative-ion sensitivities has been seen under different experimental conditions, and there can be significant complications in determining anion intensities at different pressures with trace impurity gases under chemical-ionization conditions [36].

4. Conclusions

Quantum calculations have been used to calculate electron affinities, or free energies of electron attachment, for 43 PAHs. These EA data correlate very well with reliably known experimental values and can be used, together with free energies predicted from electrochemical reduction potentials, to evaluate and confirm experimental EAs and accurately predict EAs of PAHs whose EAs have not been measured. These free energies of electron attachment have been compared with negative-ion sensitivities of PAHs, in the form of *N*/*P* ratios derived from chemical-ionization mass spectrometry. It was shown that those PAH compounds with EAs greater than 0.5 eV tend to show an enhanced signal under negative-ion CIMS over the signal in the positive-ion mode. *N*/*P* ratios for PAHs show a reasonably good correlation with EAs greater than 0.5 eV. This relationship can be used to tentatively predict *N*/*P* ratios of 15 and 600 for two carcinogenic methylbenz[*a*]anthracenes and benz[*a*]aceanthrylene, respectively.

Naphthacene and perylene are major exceptions in this relationship, with high EAs, but *N*/*P* ratios near to 1. A complete theoretical understanding of the variation in electron-attachment rates, molecular anion lifetimes, or negative-ion sensitivities has not yet been achieved at this point, but interesting features are emerging that suggest some relationship to EA and density of states in the anions, with much more work to be done theoretically to explain details and exceptions that have been noted.

Negative-ion chemical-ionization mass spectrometry should be especially useful to detect PAHs with high EAs, especially in soil and sediment matrices that are contaminated with other hydrocarbons, which will be transparent to this technique.

Notice: The U.S. EPA, through its Office of Research and Development, funded and performed the research described. This manuscript has been subjected to the EPA's peer and administrative review and has been approved for publication. Mention of trade names or commercial products does not constitute endorsement or recommendation by EPA for use.

Appendix A. Supplementary data

Supplementary data associated with this article can be found, in the online version, at doi:10.1016/j.ijms.2006.04.008.

References

[1] I. Gutman, S.J. Cyvin (Eds.), Topics in Current Chemistry: Advances in the Theory of Benenzoid Hydrocarbons, vol. 153, Springer-Verlag, New York, 1990.

[2] A.H. Neilson (Ed.), The Handbook of Environmental Chemistry: PAHs and Related Compounds. Part 1, vol. 3, Springer-Verlag, New York, 1998.

[3] Y. Kobori, S. Sekiguchi, K. Akiyama, S. Tero-Kubota, J. Phys. Chem. A 103 (1999) 5416.

[4] A. Bjørseth (Ed.), Handbook of Polycyclic Aromatic Hydrocarbons, vol. 1, Marcel Dekker Inc., New York, 1983.

[5] M.L. Lee, M.V. Novotny, K.D. Bartle, Analytical Chemistry of Polyaromatic Hydrocarbons, Academic Press, New York, 1981.

[6] Polycyclic Aromatic Hydrocarbon Carcinogenesis: Structure–Activity Relationships, CRC Press, Boca Raton, 1988.

[7] K.A.T. Berry, D.L. Burton, Can. J. Soil Sci. 77 (1997) 469.

[8] L.D. Betowski, H.M. Webb, A.D. Sauter, Biomed. Mass Spectrom. 10 (1983) 369.

[9] L.R. Hilpert, G.D. Byrd, C.R. Vogt, Anal. Chem. 56 (1984) 1842.

[10] M. Oehme, Anal. Chem. 55 (1983) 2290.

[11] (a) S. Daishima, Y. Iida, A. Shibata, F. Kanda, Org. Mass Spectrom. 27 (1992) 571;
(b) S. Daishima, Y. Iida, Chem. Lett. (1983) 273.

[12] D.H. Aue, M. Guidoni, L.D. Betowski, Int. J. Mass Spectrom. 201 (2000) 283.

[13] (a) K. Pointet, A. Milliet, S. Hoyau, M.F. Renou-Gonnord, J. Comput. Chem. 18 (1997) 629;
(b) K. Pointet, A. Milliet, M.F. Renou-Gonnord, J. Mass Spectrom. 30 (1995) 1495;
See also:
(c) O.W. Hand, B.E. Winger, R.G. Cooks, Biomed. Environ. Mass Spectrom. 16 (1989) 83.

[14] M.V. Buchanan, G. Olerich, Org. Mass Spectrom. 19 (1984) 486.

[15] A. Streitwieser Jr., Molecular Orbital Theory for Organic Chemists, Wiley, New York, 1961.

[16] L.D. Betowski, M. Enlow, L. Riddick, D.H. Aue, J. Phys. Chem. A (to be published).

[17] T. Koopmans, Physica 1 (1933) 104.

[18] A. Szabo, N.S. Ostlund, Modern Quantum Chemistry, Introduction to Advanced Electronic Structure Theory, McGraw-Hill, New York, 1989.

[19] M.J. Frisch, G.W. Trucks, H.B. Schlegel, G.E. Scuseria, M.A. Robb, J.R. Cheeseman, J.A. Montgomery Jr., T. Vreven, K.N. Kudin, J.C. Burant, J.M. Millam, S.S. Iyengar, J. Tomasi, V. Barone, B. Mennucci, M. Cossi, G. Scalmani, N. Rega, G.A. Petersson, H. Nakatsuji, M. Hada, M. Ehara, K. Toyota, R. Fukuda, J. Hasegawa, M. Ishida, T. Nakajima, Y. Honda, O. Kitao, H. Nakai, M. Klene, X. Li, J.E. Knox, H.P. Hratchian, J.B. Cross, C. Adamo, J. Jaramillo, R. Gomperts, R.E. Stratmann, O. Yazyev, A.J. Austin, R. Cammi, C. Pomelli, J.W. Ochterski, P.Y. Ayala, K. Morokuma, G.A. Voth, P. Salvador, J.J. Dannenberg, V.G. Zakrzewski, S. Dapprich, A.D. Daniels, M.C. Strain, O. Farkas, D.K. Malick, A.D. Rabuck, K. Raghavachari, J.B. Foresman, J.V. Ortiz, Q. Cui, A.G. Baboul, S. Clifford, J. Cioslowski, B.B. Stefanov, G. Liu, A. Liashenko, P. Piskorz, I. Komaromi, R.L. Martin, D.J. Fox, T. Keith, M.A. Al-Laham, C.Y. Peng, A. Nanayakkara, M. Challacombe, P.M.W. Gill, B. Johnson, W. Chen, M.W. Wong, C. Gonzalez, J.A. Pople, Gaussian 03, Revision C.02, Gaussian Inc., Pittsburgh, PA, 2003.

[20] (a) A.P. Scott, L. Radom, J. Phys. Chem. 100 (1996) 16502;
(b) D.H. Aue, J. Caras, M. Guidoni (to be published);
We have evaluated optimium scale factors for numerous PAH's and their anions and find that the DFT scale factors differ with basis set between 0.96 for the B3LYP/4-31G or 6-31G(d) levels to 0.97 for the B3LYP/6-311G(d,p) level. For thermal terms and entropies, such variation has little effect. For zero-point energies, the 0.99 scale factor fits experimental zero-point energies for unsaturated hydrocarbons reasonably well.

[21] T. Su, M.T. Bowers, Int. J. Mass Spectrom. Ion Phys. 12 (1973) 347.

[22] (a) D.K. Böhme, in: P. Ausloos (Ed.), Interaction Between Ions and Molecules, Plenum Press, NY, 1975;
(b) F. Hatch, B. Munson, J. Phys. Chem. 82 (1978) 2362;
(c) A.G. Harrison, P.H. Lin, C.W. Tsang, Int. J. Mass Spectrom. Ion Phys. 19 (1976) 23;
(d) A. Fiaux, D.L. Smith, J.H. Futrell, Int. J. Mass Spectrom. Ion Phys. 15 (1974) 9;
(e) T. Su, M.T. Bowers, J. Am. Chem. Soc. 95 (1973) 1370.

[23] (a) C.K. Mann, K.K. Barnes, Electrochemical Reactions in Nonaqueous Systems, Marcel Dekker, NY, 1970;
(b) A.J. Pappin, A.P. Tytko, K.D. Bartle, N. Taylor, D.G. Mills, Fuel 66 (1987) 1050.

[24] G.K.-C. Low, G.E. Batley, R.O. Lidgard, A.M. Duffield, Biomed. Environ. Mass Spectrom. 13 (1986) 95.

[25] K.M. Ervin, I. Anusiewicz, P. Skurski, J. Simons, W.C. Lineberger, J. Phys. Chem. A 107 (2003) 8521.

[26] W.B. Knighton, J.A. Bognar, E.P. Grimsrud, Chem. Phys. Lett. 192 (1992) 522.

[27] NIST Standard Reference Database Number 69, March 1998 Release, Negative Ion Energetics data compiled by J.E. Bartmess (http://www.webbook.nist.gov/chemistry/).

[28] P. Kebarle, S.P. Chowdhury, Chem. Rev. 87 (1987) 513.

[29] S. Chowdhury, T. Heinis, E.P. Grimsrud, P. Kebarle, J. Phys. Chem. 90 (1986) 2747.

[30] W.B. Knighton, R.S. Mock, D.S. McGrew, E.P. Grimsrud, J. Phys. Chem. 98 (1994) 3770.

[31] D.H. Williamson, W.B. Knighton, E.P. Grimsrud, Int. J. Mass Spectrom. 195/196 (2000) 481.

[32] T.M. Miller, J.M. Van Doren, A.A. Viggiano, Int. J. Mass Specrom. 233 (2004) 67.

[33] M. Lezius, Int. J. Mass Spectrom. 223/224 (2003) 447.

[34] T.M. Miller, A.A. Viggiano, A.E.S. Miller, J. Phys. Chem. A 106 (2002) 10200.

[35] S. Tobita, M. Meinke, E. Illenberger, L.G. Christophorou, H. Baumgärtel, S. Leach, Chem. Phys. 161 (1992) 501.

[36] (a) M.J. Salyards, W.B. Knighton, E.P. Grimsrud, Int. J. Mass Spectrom. 195/196 (2000) 481;
(b) W.B. Knighton, J.A. Bognar, E.P. Grimsrud, Chem. Phys. Lett. 192 (1992) 522.